

This item is the archived peer-reviewed author-version of:

De novo loss- or gain-of-function mutations in KCNA2 cause epileptic encephalopathy

Reference:

Syrbe Steffen, Hedrich Ulrike B. S., Riesch Erik, Djémié Tania, Mueller Stephan, Moller Rikke S., Maher Bridget, Hernandez-Hernandez Laura, Synofzik Matthias, Caglayan Hande S.,- De novo loss- or gain-of-function mutations in KCNA2 cause epileptic encephalopathy
Nature genetics - ISSN 1061-4036 - 47:4(2015), p. 393-399
Full text (Publisher's DOI): <https://doi.org/10.1038/NG.3239>
To cite this reference: <https://hdl.handle.net/10067/1255410151162165141>

Published in final edited form as:

Nat Genet. 2015 April ; 47(4): 393–399. doi:10.1038/ng.3239.

De novo loss- or gain-of-function mutations in *KCNA2* cause epileptic encephalopathy

Steffen Syrbe^{#1}, Ulrike B.S. Hedrich^{#2}, Erik Riesch^{#3,4,5}, Tania Djémié^{#6,7}, Stephan Müller², Rikke S. Møller^{8,9}, Bridget Maher^{10,11}, Laura Hernandez-Hernandez^{10,11}, Matthis Synofzik^{12,13}, Hande S. Caglayan¹⁴, Mutluay Arslan¹⁵, José M. Serratosa^{16,17}, Michael Nothnagel¹⁸, Patrick May¹⁹, Roland Krause¹⁹, Heidrun Löffler², Katja Detert², Thomas Dorn⁵, Heinrich Vogt⁵, Günter Krämer⁵, Ludger Schöls^{12,13}, Primus E. Mullis²⁰, Tarja Linnankivi²¹, Anna-Elina Lehesjoki^{22,23,24}, Katalin Sterbova²⁵, Dana C. Craiu^{26,27}, Dorota Hoffman-Zacharska²⁸, Christian M. Korff²⁹, Yvonne G. Weber², Maja Steinlin³⁰, Sabina Gallati⁴, Astrid Bertsche¹, Matthias K. Bernhard¹, Andreas Merkenschlager¹, Wieland Kiess¹, EuroEPINOMICS RES consortium, Michael Gonzalez³², Stephan Züchner³², Aarno Palotie^{33,34,35}, Arvid Suls^{6,7}, Peter De Jonghe^{6,7,36}, Ingo Helbig^{37,38}, Saskia Biskup³, Markus Wolff³⁹, Snezana Maljevic², Rebecca Schüle^{12,13,30}, Sanjay M. Sisodiya^{10,11}, Sarah Weckhuysen^{6,7,41}, Holger Lerche^{2,41}, and Johannes R. Lemke^{1,4,40,41}

¹Department of Women and Child Health, Hospital for Children and Adolescents, University of Leipzig, Leipzig, Germany. ²Department of Neurology and Epileptology, Hertie Institute for Clinical Brain Research, University of Tübingen, Tübingen, Germany. ³Center for Genomics and Transcriptomics (CeGaT) GmbH, Tübingen, Germany. ⁴Division of Human Genetics, University Children's Hospital Inselspital, Bern, Switzerland. ⁵Swiss Epilepsy Center, Zürich, Switzerland. ⁶Neurogenetics group, Department of Molecular Genetics, VIB, Antwerp, Belgium. ⁷Laboratory of Neurogenetics, Institute Born-Bunge, University of Antwerp, Antwerp, Belgium. ⁸Danish Epilepsy Center, Dianalund, Denmark ⁹Institute for Regional Health Services, University of Southern Denmark, Odense, Denmark. ¹⁰Department of Clinical and Experimental Epilepsy, University College London Institute of Neurology, Queen Square, London, WC1N 3BG, UK ¹¹Epilepsy Society, Chalfont-St-Peter, Bucks, SL9 0RJ, UK. ¹²Department of Neurodegenerative Diseases, Hertie Institute for Clinical Brain Research, University of Tübingen, Tübingen, Germany.

Users may view, print, copy, and download text and data-mine the content in such documents, for the purposes of academic research, subject always to the full Conditions of use:http://www.nature.com/authors/editorial_policies/license.html#terms

Correspondence: Johannes R. Lemke, MD Institut für Humangenetik Universität Leipzig Philipp-Rosenthal-Str.55 D-04103 Leipzig, Germany Tel.: +49-341-97-23800 Fax: +49-341-97-23819 johannes.lemke@medizin.uni-leipzig.de Holger Lerche, MD Abteilung Neurologie mit Schwerpunkt Epileptologie Hertie Institut für Klinische Hirnforschung Universität Tübingen Hoppe-Seyler-Str. 3 D-72076 Tübingen, Germany Tel.: +49-7071-29-80442 Fax: +49-7071-29-4488 holger.lerche@uni-tuebingen.de.

³¹Full lists of members and affiliations appear at the end of the paper.

⁴¹These authors jointly directed the work

Author contributions Study design: S.S., U.B.S.H., S.W., H.Le., J.R.L.; subject ascertainment and phenotyping: S.S., E.R., R.S.M., B.M., L.H.H., H.S.C., M.A., J.M.S., T.Do., H.V., G.K., M.Sy., L.S., P.E.M., T.L., A.-E.L., K.S., D.C., D.H.-Z., C.M.K., Y.G.W., M.St., S.G., A.B., M.K.B., A.M., W.K., A.P., A.S., P.D.J., I.H., S.B., M.W., S.M.S., S.W., H.Le., J.R.L., EuroEPINOMICS; mutation and CNV analysis: E.R., T.Dj., B.M., L.H.H., R.S., M.G., S.Z., A.S., P.D.J., S.B., S.M.S., S.W., H.Le., J.R.L.; statistical analysis: M.N., P.M., R.K., H.Le., J.R.L.; functional analysis: U.B.S.H., S.Mü., H.Lö., K.D., S.Ma., H.Le.; interpretation of data: S.S., U.B.S.H., M.W., S.Ma., S.M.S., S.W., H.Le., J.R.L.; writing manuscript: S.S., U.B.S.H., T.Dj., M.S., M.N., P.M., S.Ma., S.M.S., S.W., H.Le., J.R.L.; revising manuscript: all authors.

Competing financial interests The authors declare no competing financial interests.

Accession codes Data of the panel sequencing cohort is accessible on the GEM.app browser as "EuroEPINOMICS CH/DK cohort". Data of trio exome sequencing cohorts is accessible on the GEM.app browser as "RES EE trio sequencing" cohort.

¹³German Research Center for Neurodegenerative Diseases (DZNE), Tübingen, Germany
¹⁴Department of Molecular Biology and Genetics, Bogazici University, Istanbul, Turkey.
¹⁵Gulhane Military Medical School, Division of Child Neurology, Ankara, Turkey. ¹⁶Neurology Lab and Epilepsy Unit, Department of Neurology, IIS — Fundación Jiménez Díaz, UAM, Madrid, Spain ¹⁷Centro de Investigación Biomédica en Red de Enfermedades Raras (CIBERER), Madrid, Spain. ¹⁸Cologne Center for Genomics, University of Cologne, Cologne, Germany ¹⁹Luxembourg Centre for Systems Biomedicine (LCSB), University of Luxembourg, Esch-sur-Alzette, Luxembourg ²⁰Division of Pediatric Endocrinology, University Children's Hospital Inselspital, Bern, Switzerland. ²¹Pediatric Neurology, Children's Hospital, University of Helsinki and Helsinki University Hospital, Helsinki, Finland. ²²Folkhälsan Institute of Genetics, Helsinki, Helsinki, Finland. ²³Neuroscience Center, University of Helsinki, Helsinki, Finland ²⁴Research Program's Unit, Molecular Neurology, University of Helsinki, Helsinki, Finland ²⁵Child Neurology Department, 2nd Faculty of Medicine, Charles University, Motol Hospital, Prague, Czech Republic. ²⁶Pediatric Neurology Clinic II, Department of Neurology, Pediatric Neurology, Psychiatry, and Neurosurgery, "Carol Davila" University of Medicine, Sector 4, Bucharest, Romania. ²⁷Pediatric Neurology Clinic, "Professor Doctor Alexandru Obregia" Clinical Hospital, Sector 4, Bucharest, Romania. ²⁸Department of Medical Genetics, Institute of Mother and Child, Warsaw, Poland. ²⁹Child and Adolescent Department, Pediatric Neurology, University Hospitals, Geneva, Switzerland. ³⁰Division of Neuropediatrics, University Children's Hospital Inselspital, Bern, Switzerland. ³²Dr. JT MacDonald Department for Human Genetics, Hussman Institute for Human Genomics, University of Miami, Miami, USA ³³Institute for Molecular Medicine Finland, University of Helsinki, Helsinki, Finland ³⁴Wellcome Trust Sanger Institute, Wellcome Trust Genome Campus, Hinxton, UK. ³⁵Psychiatric & Neurodevelopmental Genetics Unit, Department of Psychiatry, Massachusetts General Hospital, Boston, MA, 02114, USA ³⁶Department of Neurology, Antwerp University Hospital, University of Antwerp, Antwerp, Belgium ³⁷Department of Neuropediatrics, Christian-Albrechts-University of Kiel, Germany. ³⁸Division of Neurology, Children's Hospital of Philadelphia, Philadelphia, USA ³⁹Department of Neuropediatrics, University of Tübingen, Tübingen, Germany. ⁴⁰Department of Diagnostics, Institute of Human Genetics, University of Leipzig, Leipzig, Germany.

These authors contributed equally to this work.

Abstract

Epileptic encephalopathies are a phenotypically and genetically heterogeneous group of severe epilepsies accompanied by intellectual disability and other neurodevelopmental features¹⁻⁶. Using next generation sequencing, we identified four different *de novo* mutations in *KCNA2*, encoding the potassium channel K_v1.2, in six patients with epileptic encephalopathy (one mutation recurred three times independently). Four individuals presented with febrile and multiple afebrile, often focal seizure types, multifocal epileptiform discharges strongly activated by sleep, mild-moderate intellectual disability, delayed speech development and sometimes ataxia. Functional studies of the two mutations associated with this phenotype revealed an almost complete loss-of-function with a dominant-negative effect. Two further individuals presented with a different and more severe epileptic encephalopathy phenotype. They carried mutations inducing a drastic gain-of-function effect leading to permanently open channels. These results establish *KCNA2* as a novel

gene involved in human neurodevelopmental disorders by two different mechanisms, predicting either hyperexcitability or electrical silencing of $K_V1.2$ -expressing neurons.

Many of the voltage-gated potassium channels (K_V1-12) are expressed in the central nervous system (CNS), playing an important role in neuronal excitability and neurotransmitter release⁷. Mutations in potassium channel-encoding genes cause different neurological diseases, including benign familial neonatal seizures (*KCNQ2/K_V7.2*, *KCNQ3/K_V7.3*)⁸⁻¹⁰, neonatal epileptic encephalopathy (*KCNQ2*)^{11,12}, episodic ataxia type 1 (EA1) (*KCNA1/K_V1.1*)¹³, and peripheral nerve hyperexcitability (*KCNA1*, *KCNQ2*)¹³⁻¹⁵. In addition, antibodies against $K_V1.1$ or associated proteins like Contactin-associated protein 2 (Caspr2) or Leucine-rich, glioma-inactivated 1 protein (LGI1) cause limbic encephalitis or neuromyotonia¹⁶. Therefore, potassium channel genes represent interesting candidates for neurodevelopmental disorders.

To identify mutations in presumed genetic forms of epilepsy, we designed a targeted re-sequencing panel¹⁷ comprising 265 known and 220 candidate genes for epilepsy (Supplementary Table 1). Screening a pilot cohort of 33 patients, we identified mutations in known epilepsy genes in 16 cases¹⁷. The remaining 17 cases were evaluated for mutations in candidate genes (Supplementary note), which led to the detection of a heterozygous *de novo* mutation in *KCNA2*, c.1214C>T, p.Pro405Leu (P405L), affecting the highly-conserved pore domain of the voltage-gated potassium channel $K_V1.2$. This mutation is not found in control databases (1000G, EVS, dbSNP138, ExAC).

The female Patient #1 carrying this mutation had unremarkable early development until epilepsy onset at 17 months old. The phenotype included febrile and afebrile alternating hemiconvulsive seizures and status epilepticus, reminiscent of Dravet syndrome. The electroencephalogram (EEG) showed multifocal spikes with marked activation during sleep. After seizure onset, ataxia and delay of psychomotor and language development became apparent. She had postnatal short stature, growth hormone deficiency and hypothyroidism. Seizures and ataxia responded poorly to antiepileptic drugs (topiramate, oxcarbazepine, valproic acid, bromide), including acetazolamide (known to be effective in EA1 caused by mutations in *KCNA1*)¹⁸. At last follow-up at eight years old, she had remained seizure-free for the past six months without previous change of medication.

Further *KCNA2* mutations were identified in several parallel studies (Supplementary Fig. 1). First, we performed whole exome sequencing (WES) in 86 parent-offspring trios with epileptic encephalopathy (31 with *SCN1A*-negative Dravet syndrome [DS], 39 with myoclonic-atonic epilepsy [MAE], and 16 with electrical status epilepticus in slow-wave sleep [ESES]). Second, we performed panel sequencing (Supplemental note) in 147 adult patients with a broad spectrum of epilepsy phenotypes associated with intellectual disability. Third, we performed WES in an adult cohort of 10 independent trios with severe epilepsy and intellectual disability, and WES in another cohort of 12 independent, isolated index cases with early-onset ataxia and epilepsy. We identified six additional independent cases with previously-unreported heterozygous *KCNA2* variants (Table 1, Supplementary note): Patient #2 (initially classified as MAE) carried the *de novo* mutation c.788T>C, p.Ile263Thr (I263T). Patient #3 (intellectual disability with neonatal-onset focal epilepsy and cerebellar

hypoplasia) carried the variant c.440G>A, p.Arg147Lys (R147K), of unknown inheritance. Since (i) it could not be confirmed as *de novo*, (ii) was predicted as benign from seven out of nine prediction tools, (iii) lysine occurs naturally at that position in drosophila and zebrafish, and (iv) did not reveal functional consequences, R147K was considered a variant of unknown significance (see Supplementary note, Supplementary Tables 1 and 2, and Supplementary Fig. 3). Patients #4 (initially classified as DS with prominent focal seizures) and #5 (intellectual disability with febrile seizures, focal seizures and status epilepticus) also carried the *de novo* P405L mutation (Fig. 1c and Supplementary Fig. 2). Patients #1, #2, #4 and #5 eventually became seizure-free between four and 15 years old, whereas intellectual disability and (in #1 and #4) mild to moderate ataxia remained unchanged. Recurrence of P405L in three independent cases suggests a mutational hotspot: c.1214 is located in a stretch of cytosines and guanines and the C>T mutation likely occurs due to a methylated CpG sequence, possibly bypassing the DNA repair system and so becoming prone to this pyrimidine-pyrimidine substitution.

Patient #6 carried the *de novo* mutation c.894G>T, p.Leu298Phe (L298F). His phenotype was different and much more severe, presenting with severe intellectual disability with gradual loss of language and motor skills, pharmaco-resistant generalized tonic-clonic, atypical absence and myoclonic seizures, facial dysmorphism, generalized epileptic discharges and moderate ataxia (Table 1 and Supplementary note). Similarly, patient #7 carrying the *de novo* mutation c.890G>A, p.Arg297Gln (R297Q) presented with a more severe phenotype consisting of moderate intellectual disability, moderate to severe ataxia and pharmaco-resistant seizures.

We subsequently screened a follow-up cohort of 99 patients, comprising 47 individuals with unresolved epileptic encephalopathy, short stature and/or ataxia as well as 52 individuals with intellectual disability and idiopathic severe GH deficiency without detecting additional sequence alterations by Sanger sequencing. We excluded copy number variations affecting *KCNA2* in all 99 follow-up cases as well as 86 trio-WES cases using an in-house-developed multiplex amplicon quantification technique (Online Methods and Supplementary Fig. 1).

To validate our findings statistically and corroborate *KCNA2* as a new disease-predisposing gene for epileptic encephalopathy, we calculated the probability for recurring *KCNA2* mutations occurring by chance in our cohorts. Comparing the allele frequency of six (two times P405L) *KCNA2* non-synonymous variants in our validation cohorts (6/(354×2), excluding the first P405L mutation detected in the discovery cohort of 33 patients) with those missense and nonsense variants reported in the largest available control database (ExAC, 144/122828), revealed a significant enrichment of *KCNA2* variants in our patient cohorts using Fisher's exact test ($p=2.6\times 10^{-4}$). Further statistical evidence is provided in the Supplementary Note. *KCNA2* had not been associated with a human disease so far.

However, during the review process of this manuscript, a single case report was published describing a 7-year-old boy with the *KCNA2* *de novo* mutation R297Q presenting with ataxia and myoclonic epilepsy, similar to our patient #7.¹⁹ In addition, the *Pingu* mouse presenting with ataxia and growth retardation carries a *Kcna2* loss-of-function mutation, p.Ile402Thr, in close proximity to P405L; *Kcna2* knock-out mice present with severe seizures and premature death^{20,21}.

K_V1.2 belongs to the K_V1 family (K_V1.1–8), all members of which are expressed in the CNS. These channels consist of four subunits with six transmembrane segments (S1–S6). S4 forms the voltage-sensor and S5–S6 the pore region containing a selectivity filter and gating ion flow²² (Fig. 1a). All four *KCNA2* sequence alterations detected in patients #1–7 (except the one in #3) are localized in highly-conserved and functionally-important protein regions (Fig. 1b), and were predicted as pathogenic. P405L disrupts the highly-conserved, K_V-specific PVP motif in S6, which is thought to link the gate to the voltage-sensor^{23,24}. A PVP>AVP mutation in K_V1.5 leads to a non-functional channel²⁵. I263T in S3 may disrupt a hydrophobic segment proposed to focus the electric field across the cell membrane, thus enabling the S4 gating charges to translocate over a smaller distance rather than the entire depth of the membrane bilayer²⁶. Furthermore, I263T in K_V1.2 corresponds to I262T in K_V1.1 causing EA1 with distal weakness.²⁷ Finally, R297Q and L298F directly affect the S4 voltage sensor, and R297Q has been described before to induce a negative shift of the activation curve.^{27,28}

Functional effects of all detected sequence alterations were examined using an automated two-microelectrode voltage-clamp oocyte testing system. We found a sigmoidal relationship between the amount of injected wildtype (WT) cRNA and potassium current amplitude, with a strong decrease in amplitude for the 8-fold cRNA amount (Fig. 2b, Supplementary Fig. 5). This quantitative titration of protein levels by varying the amounts of injected RNA was used to determine the amount of injected cRNA for further experiments. For P405L and I263T, we found a dramatic reduction of current amplitudes and thus a clear loss of channel function (Figs. 2c). When either of the two mutations were co-expressed with WT K_V1.2 in a 1:1, 1:2 or 1:4 ratio, with constant amount of injected WT cRNA, current amplitudes significantly decreased (Figs. 2d) compared with similar amounts of WT alone (Fig. 2b). Hence, both P405L and I263T exert a clear dominant-negative effect on WT K_V1.2 channels. Furthermore, I263T caused a depolarizing shift of voltage-dependent activation, and slight changes in inactivation were found for P405L (Supplementary Fig. 4).

In contrast to P405L and I263T, both R297Q and L298F induced strong gain-of-function effects. Neutralization of the second arginine in the voltage sensor in K_V1.2-R297Q increased current amplitudes by 9-fold and shifted the voltage dependence of steady-state activation by –40 mV compared with WT (Fig. 3a–c). The gain-of-function of the L298F mutation was even more pronounced with a 13-fold increase in current amplitudes and a –50 mV shift of the activation curve (Fig. 3a–c). As a consequence of the permanently open mutant channels, resting membrane potentials of oocytes expressing R297Q or L298F channels were about 40 mV more negative than of those expressing WT (Fig. 3d). Both mutations exerted a dominant effect on the WT, since co-injection of either R297Q or L298F with WT in a 0.5:0.5 ratio revealed very similar alterations as with one of the mutations (1.0) alone (Fig. 3b–d).

To examine protein production and stability, we performed SDS-page analysis of total cell lysates using a monoclonal anti-K_V1.2 antibody. Representative Western blots show that all mutations generate a protein expression level similar to the 57-kD band of the WT (Figs. 2e and 3e). A slight but reproducible shift was found for the band of P405L in both oocytes and mammalian cells (Fig. 2e, top, middle). Steric properties of proline can disrupt secondary

structure elements, which could be important for the function of the conserved PVP motif. A leucine in this position (LVP) could induce a structural change resulting in altered gel migration²⁸.

K_v1.2 belongs to the delayed rectifier class of potassium channels enabling efficient neuronal repolarization following an action potential. Loss-of-function mutations predict hyperexcitable neuronal membranes and repetitive neuronal firing due to impaired repolarization. This hypothesis is corroborated by the epileptic phenotype of the *Kcna2* knock-out mouse²¹. In stark contrast, R297Q and L298F predict permanently open channels at physiological membrane potentials, and electrical silencing by membrane hyperpolarization (as observed in oocytes). It is difficult to speculate about the pathophysiological consequences of a K_v1.2 loss- or gain-of-function beyond the level of single neurons, particularly since this channel has been detected in a broad range of both excitatory and inhibitory neurons^{29,30}. Further experiments in gene-targeted mouse models could answer these questions.

In summary, we identified *de novo* mutations in *KCNA2* causing mild to severe epileptic encephalopathy in roughly 1.7% of cases across our different cohorts. The phenotype associated with dominant-negative loss-of-function mutations comprised infantile/early-childhood seizure onset, frequent febrile and afebrile focal motor and dyscognitive seizures with overlap to DS (#1, #4, #5) and MAE (#2). However, focal seizures are uncommon in these syndromes and in particular the observed multifocal epileptiform discharges with marked activation during sleep are not described either in DS or MAE. All four patients became seizure-free between four and 15 years old with no apparent association to a recent change of medication. Thus, this improvement might either be due to a cumulative treatment response or simply represent a spontaneous resolution (Table 1, Supplementary note). Initially normal psychomotor development slowed after seizure onset, resulting in mild-moderate intellectual disability associated with mild-moderate ataxia and continuous myoclonus in some cases. By contrast, the phenotypes of patients #6 and #7, carrying mutations with dominant gain-of-function, were more severe in terms of epilepsy, ataxia and intellectual disability, and also differed electrographically, with generalized epileptic discharges. This may suggest that different pathomechanisms underlie distinctive clinical symptoms. Clinical-genetic studies and correlation with functional investigations from additional patients with further mutations are needed to confirm this genotype-phenotype relationship.

Online Methods

Whole exome and panel sequencing analysis

High throughput sequencing has been performed as described previously by our group for whole exome analysis³¹ and panel analysis¹⁷.

The panel used to screen the pilot cohort of 33 patients (including the index patient) comprised 485 known and putative epilepsy genes. (Supplementary Table 1) The candidates comprised genes that were suggestive for being involved in epileptogenesis due to several reasons, e.g. genes belong to neurotransmitter receptor families or other ion channels, genes

were discussed by different research groups as putatively involved in epilepsy, genes are associated with seizures in animals or associated with human neurodevelopmental phenotypes, etc. The gene panel used to screen the second cohort of 147 patients was an updated version of the initial panel. To improve sequence coverage and adapting the panel for purely diagnostic purposes, we excluded a few metabolic and mitochondrial genes as well as most candidate genes and added all recently published novel epileptic encephalopathy genes. This panel finally contained 280 genes including 20 candidates for research settings (Supplementary Table 2).

Sanger sequencing analysis and CNV analysis

We performed bidirectional Sanger sequencing of all three exons of *KCNA2* (ENST00000485317, NM_004974) and its intron-exon boundaries using the BigDye Terminator v3.1 Cycle Sequencing kit on an ABI3730XL DNA Analyzer (Applied Biosystems, Foster City, CA; primers available upon request) in 47 patients with epileptic encephalopathy and ataxia and/or short stature as well as 52 patients with intellectual disability and severe growth hormone deficiency.

Additionally, the genomic region containing *KCNA2* was screened for CNVs by use of an in-house-developed technique for multiplex amplicon quantification (MAQ). With this MAQ technique, we screened all 99 individuals of the Sanger sequencing cohort as well as all 86 individuals of the WES cohort (Supplementary Fig. 1). This assay comprises a multiplex PCR amplification of fluorescently-labeled target and reference amplicons, followed by fragment analysis on the ABI3730 DNA Analyzer³². The comparison of normalized peak areas between the test individual and the average of seven control individuals results in the target amplicon doses indicating the copy number of the target amplicon (using the in-house developed Multiplex Amplicon Quantification Software. The multiplex PCR reaction consists of three test amplicons located in the genomic region of *KCNA2* and three reference amplicons located on different chromosomes (primer mix is available upon request).

Pathogenicity prediction—For the prediction of the pathogenicity of nonsynonymous variants we used the ANNOVAR³³ table_annoar.pl script together with the LJB23 database (dbNSFP)³⁴ from June 2013 comprising prediction scores from SIFT, Polyphen2 (HDIV and HVAR), LRT, MutationTaster, MutationAssessor, FATHMM, MetaSVM and MetaLR scores. Scores were used as given on the ANNOVAR webpage. Additional three conservation scores (GERP+, PhyloP, SiPhy) were used to determine the conservation of a genomic position (More details in Supplementary Table 2).

Testing the enrichment of pathogenic variants—To test the enrichment of probably damaging nonsynonymous *KCNA2* variants in our data, we used the Exome Aggregation Consortium (ExAC) database as a control dataset. It comprises data from 61,486 individuals coming from various exome sequencing projects including control cohorts data but also data from studies on neurological disorders like schizophrenia and bipolar disorder. We extracted all 64 nonsynonymous (missense and nonsense) variants for *KCNA2* from ExAC [11/2014]. Some of them occurred in more than one individual yielding altogether 144 alleles with

variation in *KCNA2* out of a total number of 122828 alleles in the ExAC database. Significant enrichment of nonsynonymous variants was then tested determining the difference of allele counts in our data and the ExAC dataset using Fisher's exact test.

Probability assessment of *de novo* mutation events

We first obtained an estimate for the single-nucleotide mutation rate in the *KCNA2* gene. This rate equals the product of the average *de novo* mutation rate in humans of 1.2×10^{-8} per nucleotide per generation³⁵ and the length of the largest coding sequence of *KCNA2* (coding ID in CCDS database: 827.1) of 1,500 base pairs, yielding 1.8×10^{-5} per generation. The probability of observing a *de novo* mutation in *KCNA2* in k out of n parent-offspring trios then simply follows a binomial distribution with a success probability equaling the gene-based mutation rate, $\text{Bin}(n, k, 1.8 \times 10^{-5})$.

Functional investigations

Mutagenesis and RNA preparation—Site-directed mutagenesis was performed to engineer the mutations into the human *KCNA2* cDNA using Quickchange™ (Agilent Technologies, USA; primers are available upon request). The mutant cDNA was fully resequenced before being used in experiments to confirm the introduced mutation and exclude any additional sequence alterations. cRNA was prepared using the SP6 mMessage kit from Ambion. The human $K_V1.2$ in the pcDNA3.1 vector was kindly provided by Stephan Grissmer (Institute of Applied Physiology, Ulm University).

Electrophysiology—*Xenopus laevis* oocytes were obtained from the Institute of Physiology I, Tübingen. Preparation of the oocytes was performed as described previously¹². Oocytes were treated with collagenase (1 mg/ml of type CLS II collagenase, Biochrom KG) in OR-2 solution (in mM: 82.5 NaCl, 2.5 KCl, 1 MgCl₂ and 5 Hepes, pH 7.5) followed by three washing steps and storage at 16°C in Barth solution (in mM: 88 NaCl, 2.4 NaHCO₃, 1 KCl, 0.33 Ca(NO₃)₂, 0.41 CaCl₂, 0.82 MgSO₄ and 5 Tris/HCl, pH 7.4 with NaOH) supplemented with 50 µg/ml gentamicin (Biochrom KG). 50 nl of cRNA encoding wildtype (WT) or mutated $K_V1.2$ subunits (1 µg/µl) was injected into oocytes using the Roboocyte2 (Multi Channel Systems, Reutlingen, Germany) and stored for two days (at 17°C) prior to the experiment. Amplitudes of currents of WT and mutant channels recorded on the same day were normalized to the mean value of the 1.0 $K_V1.2$ WT on that day to pool the normalized data from different experiments together.

Automated two-electrode voltage-clamp—Potassium currents in oocytes were recorded at room temperature (20–22°C) using Roboocyte2 (Multi channel Systems, Reutlingen, Germany). For two-electrode voltage-clamp (TEVC) recordings, oocytes were impaled with two glass electrodes with a resistance of 0.4 – 1 MΩ containing 1 M KCl/ 1.5 M KAc and clamped at a holding potential of –80 mV. Oocytes were perfused with a ND96 bath solution containing (in mM): 93.5 NaCl, 2 KCl, 1.8 CaCl₂, 2 MgCl₂, 5 HEPES (pH 7.6). Currents were sampled at 5 kHz.

Voltage clamp protocols and data analysis—The membrane was depolarized to various test potentials from a holding potential of –80 mV to record potassium currents. The

activation curve (conductance–voltage relationship) was derived from the current–voltage relationship that was obtained by measuring the peak current at various step depolarizations from the holding potential of -80 mV (10 mV increment, depolarized to $+70$ mV). The following Boltzmann function was fitted to the obtained data points:

$$g(V) = \frac{g_{\max}}{\left\{1 + \exp\left[\frac{(V - V_{1/2})}{k_v}\right]\right\}}$$

with $g(V) = I/(V - V_{\text{rev}})$ being the conductance, I the recorded current amplitude at test potential V , V_{rev} the potassium reversal potential, g_{\max} the maximal conductance, $V_{1/2}$ the voltage of half-maximal activation and k_v a slope factor. Voltage-dependent inactivation of WT and mutated $K_v1.2$ channels were analyzed using 25-s conditioning pulses at potentials ranging -60 mV to 0 mV (increment 10 mV) from a holding of -80 mV, the test pulse was 30 mV. A standard Boltzmann function was fitted to the inactivation curves:

$$I(V) = \frac{I_{\max}}{\left\{1 + \exp\left[\frac{(V - V_{1/2})}{k_v}\right]\right\}}$$

with I being the recorded current amplitude at the conditioning potential V , I_{\max} being the maximal current amplitude, $V_{1/2}$ the voltage of half-maximal inactivation, and k_v a slope factor.

Western Blot Analysis—For Western blot, injected *Xenopus* oocytes were lysed in a buffer containing (in mM) 20 Tris, 100 NaCl, 1 ethylenediaminetetraacid, 0.5% Triton X-100 and 10% glycerol with protease inhibitor cOmplete (Roche, Basel, Switzerland). In addition, for the P405L mutation CHO cells were transfected with $10 \mu\text{g}/\mu\text{l}$ DNA using Mirus “TransIT®-LT1” reagent. CHO cells were lysed in a buffer containing (in M): 2 Tris (pH 7.5), 3 NaCl, 0.2 EDTA, 0.2 EGTA, 0.25 Napyrophosphate, 0.1 β -glycerolphosphate, 0.1 sodium-orthovanadate, 1 DTT, 0.1 1% Triton and 25x cOmplete solution (Roche). For measuring protein concentrations (BCA systems, Thermo Fisher Scientific) 15 – 20 μg of protein was separated by sodium dodecyl sulfate-polyacrylamide gel electrophoresis (SDS Page) on 8% polyacrylamide gels. The proteins were transferred onto polyvinylidene fluoride (PVDF) membranes (PALL Corporation, Port Washington, NY), and Western blotting was performed using a mouse-Anti- $K_v1.2$ antibody (NeuroMab clone K14/16). Water-injected oocytes, untransfected (u.t.) and water transfected (Mock) CHO cells were used as controls.

Data and statistical analysis—Sample size was estimated by using GraphPad StatMate Software. TEVC recordings were analyzed using Roboocyte 2+ (Multi Channel Systems, Germany) and Clampfit (pClamp, Axon Instruments), Origin 6.1 (Origin-Lab Corp., Northampton, USA), and Excel (Microsoft, USA) software. Data were tested for normal distribution using SigmaPlot12 (Systat Software). For statistical evaluation one-way ANOVA with Dunnett’s posthoc test (normally distributed data) or one-way ANOVA on ranks with Dunn’s posthoc test (not-normally distributed data) was used for comparing

multiple groups, with one-way ANOVA testing the overall difference between groups and posthoc tests telling the difference between specific groups. For unpaired data sets Student's t-test (normally distributed unpaired data sets) or Mann-Whitney rank-sum (not-normally distributed) were used. All data are shown as mean \pm SEM. For all statistical tests, significance with respect to control is indicated in the figures using the following symbols: * $p < 0.05$, ** $p < 0.01$, *** $p < 0.001$.

Supplementary Material

Refer to Web version on PubMed Central for supplementary material.

Acknowledgements

We thank all patients and family members for their participation in this study, Dr. S. Grissmer for providing the human cDNA clone of *KCNA2*, and Dr. F. Lang and his colleagues from the Institute of Physiology I, University of Tuebingen, for providing *Xenopus laevis* oocytes. J.R.L. (32EP30_136042 / 1), J.M.S. (EUI-EURC2011-4325), H.Le. (DFG Le1030/11-1), P.D.J. (G.A.136.11.N, FWO/ESF-ECRP), and I.H. (DFG HE 5415 3-1) received financial support within the EuroEPINOMICS-RES and -CoGIE networks (www.euroepinomics.org), a Eurocores project of the European Science Foundation. R.S. received funding from the European Union (E-Rare JTC grant 01GM1408B and PIOF-GA-2012-326681). J.M.S. received further support from the Ministerio de Economía y Competitividad (SAF2010-18586). H.Le., S.B., and S.Ma. received further support from the Federal Ministry for Education and Research (BMBF, program on rare diseases, IonNeuroNet: 01GM1105A). S.Z. received support from the NIH (R01NS072248). S.M.S. received support from the Wellcome Trust (084730), NIHR UCLH Biomedical Research Centre and Epilepsy Society, UK. M.Sy. received support by the Interdisciplinary Center for Clinical Research IZKF Tübingen (2191-0-0). A.S. received funding for a postdoctoral fellowship by the Fonds Wetenschappelijk Onderzoek. T.D. is a PhD fellow of the Institute of Science and Technology (IWT).

EuroEPINOMICS RES Consortium:

Rudi Balling¹⁹, Nina Barisic⁴³, Stéphanie Baulac⁴⁴⁻⁴⁶, Hande S Caglayan¹⁴, Dana C. Craiu^{26,27}, Peter De Jonghe^{6,7,36}, Christel Depienne^{44,46,47}, Padhraig Gormley³⁴, Renzo Guerrini⁴⁸, Ingo Helbig^{37,38}, Helle Hjalgrim⁸, Dorota Hoffman-Zacharska²⁸, Johanna Jähn³⁷, Karl Martin Klein⁴⁹, Bobby P.C. Koeleman⁵⁰, Vladimir Komarek²⁵, Roland Krause¹⁹, Eric LeGuern^{44-46,51}, Anna-Elina Lehesjoki^{22,23,24}, Johannes R. Lemke^{1,4,40}, Holger Lerche², Carla Marini⁴⁸, Patrick May¹⁹, Rikke S. Møller^{8,9}, Hiltrud Muhle³⁷, Aarno Palotie^{33,34,35}, Deb Pal⁵², Felix Rosenow⁴⁹, Kaja Selmer^{53,54}, José M. Serratosa^{16,17}, Sanjay M. Sisodiya^{10,11}, Ulrich Stephani³⁷, Katalin Sterbova²⁵, Pasquale Striano⁵⁵, Arvid Suls^{6,7}, Tiina Talvik^{56,57}, Sarah von Spiczak³⁷, Yvonne Weber², Sarah Weckhuysen^{6,7} & Federico Zara⁵⁸

⁴³Department of Paediatrics, University of Zagreb, Medical School, University Hospital Centre Zagreb, Zagreb, Croatia.

⁴⁴INSERM UMR 975, Institut du Cerveau et de la Moelle Epinière, Hôpital Pitié-Salpêtrière, Paris, France.

⁴⁵CNRS 7225, Hôpital Pitié-Salpêtrière, Paris, France.

⁴⁶Université Pierre et Marie Curie-Paris 6 (UPMC), UMRS 975, Paris, France.

⁴⁷Institut für Humangenetik, Universität Würzburg, Würzburg, Germany.

⁴⁸Pediatric Neurology Unit and Laboratories, Children's Hospital A. Meyer, University of Florence, Florence, Italy.

⁴⁹Epilepsy Center Hessen, Department of Neurology, University Hospitals Marburg and Philipps, University Marburg, Marburg, Germany.

⁵⁰Department of Medical Genetics, University Medical Center Utrecht, Utrecht, The Netherlands.

⁵¹Assistance Publique–Hôpitaux de Paris (AP-HP), Hôpital Pitié-Salpêtrière, Département de Génétique et de Cytogénétique, Unité Fonctionnelle de Neurogénétique Moléculaire et Cellulaire, Paris, France.

⁵²Department of Clinical Neuroscience, Institute of Psychiatry, King's College London, London, UK.

⁵³Department of Medical Genetics, Oslo University Hospital, Oslo, Norway.

⁵⁴Institute of Medical Genetics, University of Oslo, Oslo, Norway.

⁵⁵Pediatric Neurology and Muscular Diseases Unit, Department of Neurosciences, Rehabilitation, Ophthalmology, Genetics, Maternal and Child Health, 'G Gaslini Institute', Genova, Italy.

⁵⁶Department of Pediatrics, University of Tartu, Tartu, Estonia.

⁵⁷Department of Neurology and Neurorehabilitation, Children's Clinic, Tartu University Hospital, Tartu, Estonia.

⁵⁸Laboratory of Neurogenetics, Department of Neurosciences, Gaslini Institute, Genova, Italy.

URLs.

dbSNP Build 138, <http://www.ncbi.nlm.nih.gov/projects/SNP/>; 1000 Genomes Project database, <http://www.1000genomes.org/>; Exome Variant Server, <http://evs.gs.washington.edu/EVS/>; ExAC, <http://exac.broadinstitute.org/>; PolyPhen-2, <http://genetics.bwh.harvard.edu/pph2/>; MutationTaster, <http://www.mutationtaster.org/>; Multiplex Amplicon Quantification, <http://www.multiplicom.com/multiplex-amplicon-quantification-maq>; Multiplex Amplicon Quantification Software, <http://www.multiplicom.com/maq-s>; ANNOVAR, http://www.openbioinformatics.org/annovar/annovar_filter.html#ljb23; GEM.app browser, <https://genomics.med.miami.edu/>.

References

1. Capovilla G, Wolf P, Beccaria F, Avanzini G. The history of the concept of epileptic encephalopathy. *Epilepsia*. 2013; 54(Suppl 8):2–5.
2. Guerrini R, Pellock JM. Age-related epileptic encephalopathies. *Handb Clin Neurol*. 2012; 107:179–93. [PubMed: 22938971]

3. Claes L, et al. *De novo* mutations in the sodium-channel gene *SCN1A* cause severe myoclonic epilepsy of infancy. *Am J Hum Genet.* 2001; 68:1327–32. [PubMed: 11359211]
4. Nava C, et al. *De novo* mutations in *HCN1* cause early infantile epileptic encephalopathy. *Nat Genet.* 2014; 46:640–5. [PubMed: 24747641]
5. Epi KC, et al. *De novo* mutations in epileptic encephalopathies. *Nature.* 2013; 501:217–21. [PubMed: 23934111]
6. Lerche H, et al. Ion channels in genetic and acquired forms of epilepsy. *J Physiol.* 2013; 591:753–64. [PubMed: 23090947]
7. Lai HC, Jan LY. The distribution and targeting of neuronal voltage-gated ion channels. *Nature Reviews Neuroscience.* 2006; 7:548–562. [PubMed: 16791144]
8. Biervert C, et al. A potassium channel mutation in neonatal human epilepsy. *Science.* 1998; 279:403–6. [PubMed: 9430594]
9. Charlier C, et al. A pore mutation in a novel KQT-like potassium channel gene in an idiopathic epilepsy family. *Nat Genet.* 1998; 18:53–5. [PubMed: 9425900]
10. Singh NA, et al. A novel potassium channel gene, *KCNQ2*, is mutated in an inherited epilepsy of newborns. *Nat Genet.* 1998; 18:25–9. [PubMed: 9425895]
11. Weckhuysen S, et al. *KCNQ2* encephalopathy: emerging phenotype of a neonatal epileptic encephalopathy. *Ann Neurol.* 2012; 71:15–25. [PubMed: 22275249]
12. Orhan G, et al. Dominant-negative effects of *KCNQ2* mutations are associated with epileptic encephalopathy. *Ann Neurol.* 2014; 75:382–94. [PubMed: 24318194]
13. Browne DL, et al. Episodic ataxia/myokymia syndrome is associated with point mutations in the human potassium channel gene, *KCNA1*. *Nat Genet.* 1994; 8:136–40. [PubMed: 7842011]
14. Wuttke TV, et al. Peripheral nerve hyperexcitability due to dominant-negative *KCNQ2* mutations. *Neurology.* 2007; 69:2045–53. [PubMed: 17872363]
15. Dedek K, et al. Myokymia and neonatal epilepsy caused by a mutation in the voltage sensor of the *KCNQ2* K⁺ channel. *Proc Natl Acad Sci U S A.* 2001; 98:12272–7. [PubMed: 11572947]
16. Irani SR, et al. Antibodies to K_v1 potassium channel-complex proteins leucine-rich, glioma inactivated 1 protein and contactin-associated protein-2 in limbic encephalitis, Morvan's syndrome and acquired neuromyotonia. *Brain.* 2010; 133:2734–48. [PubMed: 20663977]
17. Lemke JR, et al. Targeted next generation sequencing as a diagnostic tool in epileptic disorders. *Epilepsia.* 2012; 53:1387–98. [PubMed: 22612257]
18. Lubbers WJ, et al. Hereditary myokymia and paroxysmal ataxia linked to chromosome 12 is responsive to acetazolamide. *J Neurol Neurosurg Psychiatry.* 1995; 59:400–5. [PubMed: 7561920]
19. Pena SD, Coimbra RL. Ataxia and myoclonic epilepsy due to a heterozygous new mutation in *KCNA2*: proposal for a new channelopathy. *Clin Genet.* 2015; 87:e1–3. [PubMed: 25477152]
20. Xie G, et al. A new K_v1.2 channelopathy underlying cerebellar ataxia. *J Biol Chem.* 2010; 285:32160–73. [PubMed: 20696761]
21. Brew HM, et al. Seizures and reduced life span in mice lacking the potassium channel subunit K_v1.2, but hypoexcitability and enlarged K_v1 currents in auditory neurons. *J Neurophysiol.* 2007; 98:1501–25. [PubMed: 17634333]
22. Jan LY, Jan YN. Voltage-gated potassium channels and the diversity of electrical signalling. *J Physiol.* 2012; 590:2591–9. [PubMed: 22431339]
23. Holmgren M, Shin KS, Yellen G. The activation gate of a voltage-gated K⁺ channel can be trapped in the open state by an intersubunit metal bridge. *Neuron.* 1998; 21:617–21. [PubMed: 9768847]
24. Long SB, Campbell EB, Mackinnon R. Voltage sensor of K_v1.2: structural basis of electromechanical coupling. *Science.* 2005; 309:903–8. [PubMed: 16002579]
25. Labro AJ, Raes AL, Bellens I, Ottschytch N, Snyders DJ. Gating of shaker-type channels requires the flexibility of S6 caused by prolines. *J Biol Chem.* 2003; 278:50724–31. [PubMed: 13679372]
26. Chen X, Wang Q, Ni F, Ma J. Structure of the full-length Shaker potassium channel K_v1.2 by normal-mode-based X-ray crystallographic refinement. *Proc Natl Acad Sci U S A.* 2010; 107:11352–7. [PubMed: 20534430]

27. Klein A, Boltshauser E, Jen J, Baloh RW. Episodic ataxia type 1 with distal weakness: a novel manifestation of a potassium channelopathy. *Neuropediatrics*. 2004; 35:147–9. [PubMed: 15127317]
28. Nybo K. Molecular biology techniques Q&A. Western blot: protein migration. *Biotechniques*. 2012; 53:23–4. [PubMed: 22780315]
29. Lorincz A, Nusser Z. Cell-type-dependent molecular composition of the axon initial segment. *J Neurosci*. 2008; 28:14329–40. [PubMed: 19118165]
30. Wang H, Kunkel DD, Schwartzkroin PA, Tempel BL. Localization of Kv1.1 and Kv1.2, two K channel proteins, to synaptic terminals, somata, and dendrites in the mouse brain. *J Neurosci*. 1994; 14:4588–99. [PubMed: 8046438]
31. Suls A, et al. De novo loss-of-function mutations in CHD2 cause a fever-sensitive myoclonic epileptic encephalopathy sharing features with Dravet syndrome. *Am J Hum Genet*. 2013; 93:967–75. [PubMed: 24207121]
32. Suls A, et al. Microdeletions involving the SCN1A gene may be common in SCN1A-mutation-negative SMEI patients. *Hum Mutat*. 2006; 27:914–20. [PubMed: 16865694]
33. Wang H, Kunkel DD, Martin TM, Schwartzkroin PA, Tempel BL. Heteromultimeric K⁺ channels in terminal and juxtapanodal regions of neurons. *Nature*. 1993; 365:75–9. [PubMed: 8361541]
34. Liu X, Jian X, Boerwinkle E. dbNSFP v2.0: a database of human non-synonymous SNVs and their functional predictions and annotations. *Hum Mutat*. 2013; 34:E2393–402. [PubMed: 23843252]
35. Kong A, et al. Rate of *de novo* mutations and the importance of father's age to disease risk. *Nature*. 2012; 488:471–5. [PubMed: 22914163]

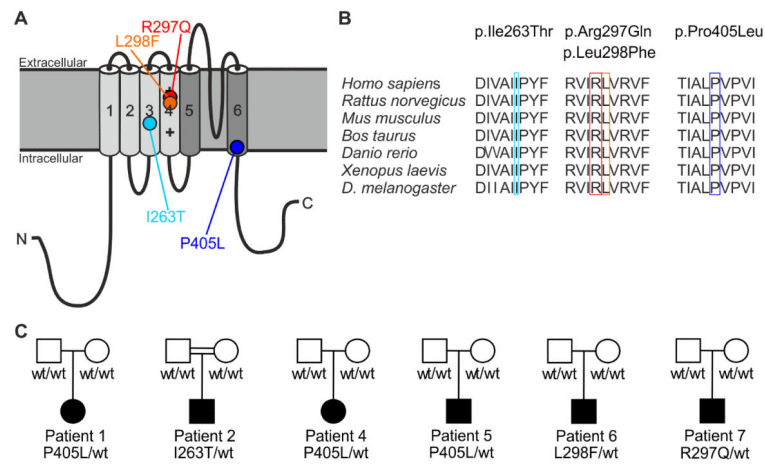
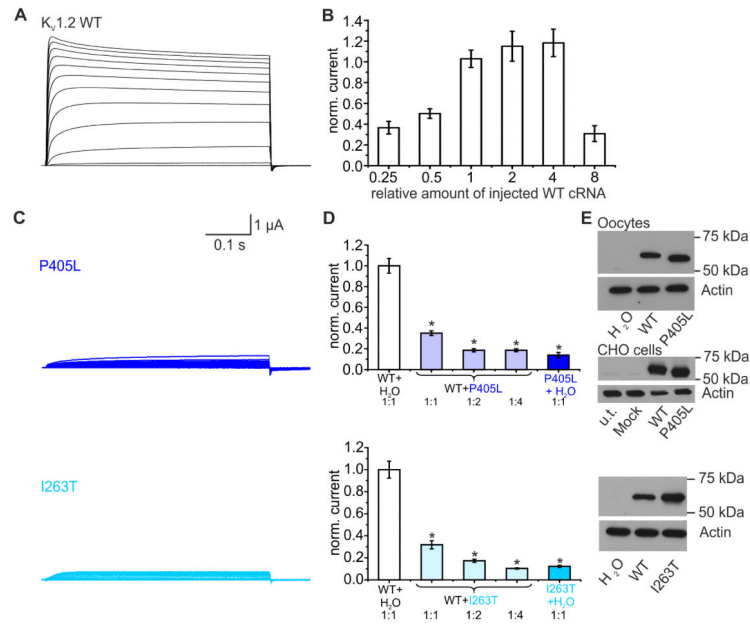


Figure 1. Mutations in the $K_V1.2$ channel. **(A)** Structure of the voltage-gated potassium channel $K_V1.2$ with transmembrane segments S1–S4 forming the voltage sensor domain (light gray) and the pore region S5–S6 (in dark gray) with its pore-forming loop. Mutations are localized in highly-conserved regions in the S3 segment (I263T, light blue), the S4 segment constituting the voltage sensor (R297Q, red; L298F, orange) and the S6 segment (P405L, dark blue). **(B)** I263, R297, L298 and P405 and the respective surrounding amino acids show evolutionary conservation. **(C)** Pedigrees of patients #1, #2 and #4–7.

**Figure 2.**

Functional effects of the *KCNA2* mutations P405L and I263T. **(A)** Representative current traces of $K_{V1.2}$ wildtype (WT) channels recorded in a *Xenopus laevis* oocyte during voltage steps (from -80 mV to $+70$ mV). **(B)** Effect of increasing amounts of injected WT-*KCNA2* cRNA on current amplitude (0.25: $n=13$; 0.5: $n=18$; 1: $n=22$; 2: $n=17$; 4: $n=20$; 8: $n=19$). Shown are means \pm SEM. **(C)** Current traces derived from $K_{V1.2}$ -P405L (top) and $K_{V1.2}$ -I263T (bottom) channels recorded as described in (A). **(D)** K^+ -currents were reduced for mutants P405L (top) and I263T (bottom) compared to WT-cRNA (top: P405L: $n=10$; WT: $n=44$; bottom: I263T: $n=10$; WT: $n=34$). A dominant-negative effect of P405L and I263T mutants on $K_{V1.2}$ -WT channels was shown when a constant amount of WT cRNA (amount 1 in (B)) was injected with either H_2O or increasing amounts of mutant cRNA (top: P405L: ratio 1:1: $n=47$; ratio 1:2: $n=40$; ratio 1:4: $n=36$; bottom: I263T: ratio 1:1: $n=34$; ratio 1:2: $n=42$; ratio 1:4: $n=38$). Co-expression of P405L or I263T and the WT led to a significant reduction of the current amplitude compared to the WT alone. Groups were statistically different (One-way ANOVA ($p<0.001$), posthoc Dunn's method ($p<0.05$)). Shown are means \pm SEM. **(E)** Western blot analysis from lysates of *Xenopus laevis* oocytes injected with equal amounts of $K_{V1.2}$ -WT or mutant cRNA (P405L: top; I263T: bottom) or from lysates of CHO cells transiently transfected with $K_{V1.2}$ -WT and P405L cDNAs (middle). For P405L-mutant channels there was a shift from 57 kDa to ~ 58.5 kDa ($n=3$). $K_{V1.2}$ -WT or I263T ($n=3$) mutant channels revealed similar bands (57 kDa).

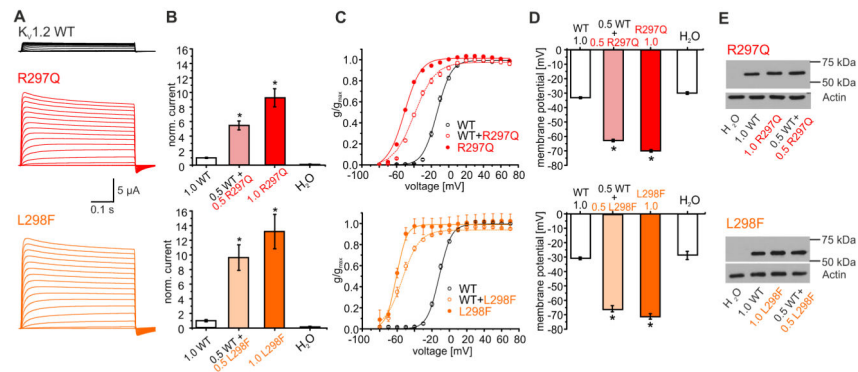


Figure 3.

Functional effects of the $K_V1.2$ mutations R297Q and L298F. **(A)** Representative current traces derived from $K_V1.2$ -WT (top), R297Q (middle) or L298F mutant channels (bottom) recorded as described in Fig. 2A. **(B)** Mean current amplitudes of top: $K_V1.2$ -WT (1.0, $n=23$), WT + R297Q (0.5:0.5, $n=37$), R297Q (1.0, $n=35$) and H_2O injection ($n=25$); bottom: $K_V1.2$ -WT (1.0, $n=13$), WT + L298F (0.5:0.5, $n=26$), L298F (1.0, $n=14$), and H_2O injection ($n=10$). Shown are means \pm SEM. There was a statistical significant difference between WT and tested groups (ANOVA on ranks; $p<0.001$) with posthoc Dunn's Method ($p<0.05$). **(C)** Mean voltage dependence of $K_V1.2$ channel activation for WT, R297Q (red, top) or L298F channels (orange, bottom). Shown are means \pm SEM. Lines represent Boltzmann functions fit to data points. Activation curves of mutant channels were significantly shifted to more hyperpolarized potentials ($p<0.05$). For details see Supplementary notes. **(D)** Resting membrane potentials of oocytes injected with: top: WT (1.0, $n=44$), WT+R297Q (0.5:0.5, $n=42$), R297Q (1.0; $n=38$) or H_2O ($n=24$); bottom: WT (1.0, $n=30$), WT+L298F (0.5:0.5, $n=34$), L298F (1.0; $n=28$) or H_2O ($n=13$). Shown are means \pm SEM. Statistically significant differences between WT and tested groups was verified by ANOVA on ranks ($p<0.001$) with posthoc Dunn's Method ($p<0.05$). **(E)** Western blot analysis from lysates of *Xenopus* oocytes injected with $K_V1.2$ -WT (1.0), $K_V1.2$ -WT (0.5) + R297Q (0.5, top), mutant R297Q (1.0, top), $K_V1.2$ -WT (0.5) + L298F (0.5, bottom) or mutant L298F (1.0, bottom) cRNA ($n=3$). All channels revealed similar bands (57 kDa).

Table 1

Main phenotypic characteristics of patients carrying a disease-causing *de novo* *KCNA2* mutation.

	Patient 1	Patient 2	Patient 4	Patient 5	Patient 6	Patient 7
Cohort	1 st epilepsy panel (n=33)	MAE (n=39)	DS (n=31)	adult EE I (n=147)	adult EE II (n=10)	Ataxia & epilepsy (n=12)
Mutation	c.1214C>T, p.Pro405Leu <i>de novo</i>	c.788T>C, p.Ile263Thr <i>de novo</i>	c.1214C>T, p.Pro405Leu <i>de novo</i>	c.1214C>T, p.Pro405Leu <i>de novo</i>	c.894G>T, p.Leu298Phe <i>de novo</i>	c.890G>A, p.Arg297Gln <i>de novo</i>
Functional consequence	loss of function				gain of function	
Gender/Age	F/8y	M/7y	F/5y	M/19y	M/36y	M/26y
Development prior to seizure onset	normal					
Age at seizure onset	17m	11m	10m	8m	6m	5m
Seizure type at onset	FS, hemiclonic seizures	MC	FS, FDS	Febrile SE	GTCS	Febrile SE
Other seizure types	FS, MC, FDS, focal motor seizures, secondary GTCS	MC, MA	FS, FDS, focal motor seizures, possible extension spasms	FS, focal motor seizures, secondary GTCS	MC, atypical absences	GTCS, absences
Seizure outcome	Seizure free since age 7 ½y old	Seizure free since age 4y old	Seizure free since age 4y old	Seizure free since age 15y old	GTCS bimonthly on polytherapy	GTCS once a year on lamotrigine
EEG at onset	Focal sharp waves	Focal sharp waves and spikes	normal	Sharp waves, bilateral centro-temporo-frontal spikes	n.a.	n.a.
Course of EEG	Multifocal sharp waves and sharp slow waves, accentuated over the left frontocentral region with significant increase during sleep	Multifocal sharp waves and polyspikes. Since age 6y: normal	Focal sharp waves. From age 2y: sharp waves, spike-waves and polyspike-waves over both centro-temporal regions, independently or bilaterally synchronous (left more than right); increase during sleep	At age 4y: multifocal epileptiform discharges activated by sleep. Since age 17y: normal	At age 22y: frequent generalized spike wave discharges in a diffusely slow background	At age 6y: generalized spike waves and polyspike-waves
Neurological examination	Mild-moderate ataxia, constant myoclonus	normal	Mild ataxia, myoclonus at rest in hand and fingers	normal	Moderate ataxia, occasional myoclonus at rest	Moderate-severe ataxia, hyperreflexia
Development at last follow up	Mild-moderate ID, delayed speech development	Mild-moderate ID	Learning disability, delayed speech development	Moderate ID, delayed speech development	Severe ID, no speech, requires help with all aspects of daily activities	Moderate ID
MRI	normal					
Additional features	GH deficiency, IGF-1: -0.7 SDS (1y2m), -8.5 SDS (3y5m) subclinical hypothyroidism			Severe scoliosis	Facial dysmorphism (broad forehead, bulbous nasal tip, deep set eyes, synophris, full lips)	

Abbreviations: F: female; FDS: focal dyscognitive seizures; FS: febrile seizures; GH: growth hormone; GTCS: generalized tonic-clonic seizures; ID: intellectual disability; HC: head circumference; m: months; M: male; MA: myoclonic-atic seizures; MC: myoclonic seizures; n.a.: not available; SE: status epilepticus; y: years